JOURNAL OF VIROLOGY, Sept. 2007, p. 9502–9511 Vol. 81, No. 17
0022-538X/07/$08.00+0 doi:10.1128/JVI.00208-07

Local Expression of Secondary Lymphoid Tissue Chemokine Delivered by Adeno-Associated Virus within the Tumor Bed Stimulates Strong Anti-Liver Tumor Immunity▽

Chun-min Liang,[1,2] Cui-ping Zhong,[1] Rui-xia Sun,[2] Bin-bin Liu,[2] Cheng Huang,[2] Jie Qin,[1] Shuang Zhou,[1] Junling Shan,[1] Yin-kun Liu,[2] and Sheng-long Ye[2]*

Department of Anatomy and Histology and Embryology, Shanghai Medical College, Fudan University, 200032 Shanghai, People's Republic of China,[1] and Liver Cancer Institute of Zhongshan Hospital, Fudan University, 200032 Shanghai, People's Republic of China[2]

Received 30 January 2007/Accepted 30 May 2007

Development of an effective antitumor immune response depends on the appropriate interaction of effector and target cells. Thus, the expression of chemokines within the tumor may induce a more potent antitumor immune response. Secondary lymphoid tissue chemokine (SLC) is known to play a critical role in establishing a functional microenvironment in secondary lymphoid tissues. Its capacity to attract dendritic cells (DCs) and colocalize them with T cells makes it a good therapeutic candidate against cancer. In this study, we used SLC as a treatment for tumors established from a murine hepatocellular carcinoma model. SLC was encoded by recombinant adeno-associated virus (rAAV), a system chosen for the low host immunity and high efficiency of transduction, enabling long-term expression of the gene of interest. As a result, rAAV-SLC induced a significant delay of tumor progression, which was paralleled by a profound infiltration of DCs and activated $CD4^+$ T cells and $CD8^+$ T cells ($CD3^+$ $CD69^+$ cells) into the tumor site. In addition, rAAV-SLC treatment was also found to reduce tumor growth in nude mice, most likely due to inhibition of neoangiogenesis. In conclusion, local expression of SLC by rAAV represents a promising approach to induce immune-mediated regression of malignant tumors.

The genetic modification of tumor cells, e.g., with cytokine genes, represents a rational approach to modify the tumor microenvironment that favors innate or adaptive immunity to prevent or reverse tumor development. In particular, chemokine gene transfer offers the possibility to trigger the recruitment of initiators and/or effectors of the immune response directly to the tumor microenvironment. The generation of an antitumor immune response is a complex process dependent on coordinate interaction of different subsets of effector cells, including both antigen-presenting cells (APCs) and lymphocyte effectors (18). Secondary lymphoid tissue chemokine (SLC), also called 6Ckine or CCL21, is expressed in high endothelial venules (HEVs), the main port of lymphocyte entry into peripheral lymph nodes, in the T-cell areas of lymph node, spleen, and Peyer's patches (13, 17, 28, 50). CC chemokine receptor 7 (CCR7), the principal SLC receptor, has been shown to play an important role in establishing the functional microenvironment of secondary lymphoid tissues (5, 6, 12, 13, 17, 23, 27, 28, 33, 50, 56). In addition to CCR7, SLC also interacts with CXCR3, through which it can block angiogenesis in vivo (41). Previous data have established that SLC exerts potent chemotactic activity on dendritic cells (DCs), T cells, and B cells; thus, it might be used to generate an antitumor immune response (38, 39, 44, 47). Accordingly, intratumoral injection of SLC as well as intratumoral injection of SLC-gene-modified DCs (55) induced antitumor activity. However, these effects were limited, suggesting that the antitumoral response was not sufficiently robust. One might speculate that a stronger response could be induced by attracting larger numbers of effector T cells and APCs to the site of tumor. This would require that a more efficient expression system be established to produce SLC in the tumor bed.

The efficiency of an expression vector is one of the key considerations for gene therapy. A vast majority of these approaches have been attempted using adenoviral vectors and, to a lesser extent, retroviral vectors. The major limitation of adenoviruses is their induction of an inflammatory response and the temporally limited production of the gene of interest. Thus, a successful therapeutic outcome can only be achieved by efficient infection of target tissues and the establishment of long-term gene expression. Recently, recombinant adeno-associated viruses (rAAV) have emerged as promising nonpathogenic vectors with a potential for cancer gene therapy. rAAV can successfully infect and transduce a broad variety of cell and tissue types, such as brain, liver, and muscle (4, 9, 22, 52). Transduction with rAAV results in a low-level inflammatory response and enables long-term expression of the gene of interest. In vivo studies using rAAV have already demonstrated beneficial therapeutic effects in the treatment of various diseases in animal models and in human clinical trials (25, 42). Moreover, rAAV vectors have been proven to be capable of inducing antitumor effects in vivo (7, 15, 51). In this study, we evaluated the potential of rAAV for in vivo SLC gene modification of tumors and tested its antitumor properties. This is

* Corresponding author. Mailing address: Liver Cancer Institute of Zhongshan Hospital, Fudan University, 200032 Shanghai, People's Republic of China. Phone: 86 21 64041990 2150. Fax: 86 21 64037181. E-mail: slye@shmu.edu.cn.

▽ Published ahead of print on 13 June 2007.

the first report of genetic modification of tumor cells to express SLC using rAAV serotype 2 as the delivery vector. This report demonstrates that SLC gene transfer significantly decreases the tumorigenesis of the Hepal-6 liver cancer cell line by inducing both activated, T-cell-mediated tumor resistance and inhibition of angiogenesis.

MATERIALS AND METHODS

Animals. C57BL/6J (H-2^b), BALB/c (H-2^d), and female nude mice (6 to 8 weeks of age) were purchased from the Chinese Academy of Science and housed at the Animal Maintenance Facility of the Shanghai Medical College, Fudan University.

Medium and chemokines. Complete medium consisted of RPMI 1640 medium supplemented with 10% heat-inactivated fetal calf serum, 0.1 mM nonessential amino acids, 1 μM sodium pyruvate, 2 mM fresh L-glutamine, 100 μg/ml streptomycin, 100 units/ml penicillin, 50 μg/ml gentamicin, and 0.5 μg/ml fungizone. Serum-free Opti-MEM I medium was obtained from GIBCO-BRL (Gaithersburg, MD). Recombinant murine SLC was sourced from BIodesign (Saco, ME); rat anti-mouse SLC antibody was purchased from eBioScience company (San Diego, CA).

Tumor cell lines. The murine Hepal-6 hepatocellular carcinoma cell line (ATCC CRL-1830) was purchased from the Chinese Academy of Sciences. AAV293 cells were purchased from Stratagene (La Jolla, CA).

Production and purification of rAAV-SLC. The AAV Helper-Free System (Stratagene) was used for rAAV serotype 2 packaging. To amplify fragments containing the full coding region, the following specific primers for murine SLC were used: 5′-AGCGAATTCTACAGCTCTGGTCTCATCCTCA-3′ (sense) and 5′-GCGCTCGAGGTCTCTTTTCTAGCTCCCTCTTTG-3′ (antisense), containing EcoRI or XhoI sites, respectively. Total cellular RNA was extracted from C57BL/6J mice lymph nodes. The above fragments were amplified using a reverse transcription-PCR (RT-PCR) kit (QIAGEN, Germany). After the entire nucleotide sequences of the PCR products were confirmed, the EcoRI-XhoI fragment was inserted into the multiple cloning sites of pAAV-IRES-hrGFP (where IRES is internal ribosome entry site and hrGFP is humanized recombinant green fluorescent protein) which features a cytomegalovirus (CMV) promoter and AAV2 inverted terminal repeats. rAAV-SLC serotype 2 vectors were packaged in AAV293 cells using the three-plasmid cotransfection system (26). hrGFP expression was used to ascertain the infection efficiency. AAV293 cells were harvested 72 h posttransfection and lysed by repeated freezing and thawing. DNase I treatment of viral preparations was performed to digest unencapsidated DNA before real-time quantitative PCR (QIAGEN, Germany) analysis was used to determine the particle genome titer.

CMV promoter-specific quantitative real-time quantitative PCR for determining titer. PCR was performed as previously reported (34), using the FastStart DNA Master SYBR Green system (Roche Molecular Biochemicals, Mannheim, Germany). The following primers were used: CMV forward, 5′-GGCGGAGTT GTTACGACAT-3′; CMV reverse, 5′-GGGACTTTCCCTACTTGGCA-3′. A fragment length of 201 bp is expected for the quantitative PCR product using these primers. PCR was carried out in a final volume of 20 ml using 0.8 ml of each primer (0.4 mM), 3.2 ml $MgCl_2$ (25 mM), 2 ml of the supplied enzyme mix, 11.2 ml of H_2O, and finally 2 ml of the template. The enzyme mix contained the reaction buffer, Fast-Start *Taq* DNA polymerase, and the double-stranded DNA-specific SYBR Green I dye for detection of PCR products. PCR was performed with a 10-min preincubation at 95.8°C, followed by 50 cycles of 15 s at 95.8°C (denaturation), 5 s at 67.8°C (annealing), and 10 s at 72.8°C (extension). PCR products were subjected to melting curve analysis using a light cycler system to exclude the amplification of nonspecific products. Finally, the PCR products were analyzed by conventional agarose gel electrophoresis.

Viral transduction. At 24 h before transfection, Hepal-6 cells were plated in growth medium without antibiotics and grown to 80 to ~90% confluence. The cells were washed once with Opti-MEM I medium and incubated with rAAV2 at a multiplicity of infection of 100 for 2 h at 37°C with 7% CO_2 and gentle agitation every 15 min. After infection, cells were washed three times with serum-free Opti-MEM and cultured in complete RPMI medium until further analysis.

Monitoring the intracellular distribution of rAAV-SLC. To investigate the infectious entry pathway of rAAV-SLC and assess AAV-mediated gene transfer, purified virus was labeled with the carbocyanine dye Cy3 (Amersham, NJ). Cy3-labeled AAV (Cy3-AAV) was prepared as previously described (36). Hepal-6 cells were infected with 1×10^{11} particles/ml of Cy3-conjugated rAAV (approximately 10^6 particles/cell) in binding buffer (Dulbecco's modified Eagle's medium containing 2 mM glucose, 10 mM HEPES [pH 7.3], and 1% bovine serum albumin) at 37°C unless otherwise noted. Cells were washed three times with binding buffer prior to infection. Prior to fixation, the binding buffer was removed, and the cells were washed three times. Cells were then fixed with 4% paraformaldehyde in phosphate-buffered saline (PBS) for 15 min at room temperature and washed three times with PBS. Where indicated, cells were either treated for 5 min at room temperature with 1-μg/ml 4′,6′-diamidino-2-phenylindole (DAPI) (Invitrogen, Eugene, OR) in PBS with 0.1% Triton X-100 and washed three times with PBS or mounted in medium containing DAPI, which was used to indicate the position of the cell nucleus. Distribution of Cy3-AAV particles in Hepal-6 cells 2 h postinfection was analyzed by confocal microscopy 2 h postinfection.

Detection of SLC produced by Hepal-6 cells infected with rAAV-SLC. SLC expression from Hepal-6 cells posttransfection was confirmed by RT-PCR and by specific enzyme-linked immunosorbent assay (ELISA). Supernatants were collected from the cultured Hepal-6 cells that were treated with either rAAV-GFP or rAAV-SLC at 24, 48, and 72 h postinfection and stored at −76°C for further use. At the same time points, total RNA was also extracted from these cultured Hepal-6 cells for RT-PCR analysis. A chemotaxis assay was used to further determine the bioactivity of the SLC produced in the supernatant of SLC-transduced Hepal-6 cells. For the chemoattractant source, supernatants from infected cells were added to the bottom chamber of 24-well plates with a 6.5-mm diameter and 5-μm-pore-size polycarbonate transwell insets (Corning Coster, Cambridge, MA) in quadruplicate. T cells were purified from normal C57BL/6J mouse spleen as responder cells, using a mouse T-cell recovery column kit (Cedarlane, Ontario, Canada) according to the manufacturer's instructions.

Determination of cell viability by dye exclusion assay and methylthiazol tetrazolium (MTT) assay. Viable cell ratios were determined using a dye exclusion assay. This assay is based on the exclusion of trypan blue dye from viable cells. Transfected cells were collected at 24, 48, and 72 h postinfection and then incubated with 0.4% trypan blue (Sigma) for 5 min. Cells were then observed under a microscope and counted as stained or nonstained on a hemocytometer. From this, viable cell ratios were calculated according to the following formula: percent viable cell ratio = (number of nonstained cells/total number of cells) × 100%.

Meanwhile, the cell viability of transfected cells was measured by MTT assay. At 24, 48, and 72 h postinfection, cells were plated in 96-well plates, and then 100 μl of MTT was added to each well of the plates and incubated at 37°C for 4 h. Medium was then aspirated and replaced with 100 μl of dimethyl sulfoxide (Sigma) to solubilize crystals. Spectrophotometric absorbance of each sample was measured at 450 nm using a Spectra microplate reader (Bio-Rad) against a blank prepared from cell-free wells. Cell survival was expressed as a fraction of the number of cells in untreated controls.

Tumor establishment in C57BL/6J mice. A total of 1×10^6 infected or noninfected Hepal-6 cells diluted in 200 μl of serum-free RPMI 1640 medium were injected subcutaneously (s.c.) into the left flank of 6- to 8-week-old C57BL/6J mice to inoculate tumors. Tumor-bearing mice were divided into different groups: (i) control tumor-bearing mice, injected with noninfected Hepal-6 cells to inoculate tumors; (ii) rAAV-GFP transfected tumor-bearing mice, injected with Hepal-6 cells 48 h postinfection with rAAV-GFP; and (iii) rAAV-SLC-transfected tumor-bearing mice, injected with Hepal-6 cells 48 h postinfection with rAAV-SLC. After the tumors had grown to a size of 8 mm^3, control tumor-bearing mice also received three different treatments as follows: (iv) PBS group, intratumoral injection with PBS; (v) rAAV-GFP injection group, intratumoral injection with mock rAAV-GFP vectors (5 μl; 0.6×10^9 viral particles); and (vi) rAAV-SLC injection group, intratumoral injection with rAAV-SLC vectors (5 μl, or 0.6×10^9 viral particles). As previously indicated, the AAV viral vectors were delivered to six sites, 0.5 mm apart, along the needle track as the needle was withdrawn, with a volume of approximately 0.8 μl at each of the six sites over 10 min. The needle was left in the tissue for an additional 5 min and then was slowly withdrawn. Developing tumors were then monitored twice weekly by palpation measurement of tumor diameter for 40 days. Tumor volume (in cubic millimeters) was calculated by the formula: volume = 0.4 × longest diameter × shortest diameter.

IHC analysis for expression of SLC in tumor sites. For immunohistochemical (IHC) analysis of SLC expression in tumor sites, tumors were harvested at day of 20 and embedded in 22-oxyacalcitriol (OCT) compound (Torrance, CA) before being snap frozen in liquid nitrogen and stored at −76°C until IHC procedures were performed. Serial 5-μm-thick cryostat sections were incubated with anti-mSLC (PeproTech Inc.) and amplified using a Cy3-streptavidin ABC system (Santa Cruz Biotechnology).

IHC analysis and flow cytometry for infiltration of $CD11c^+$ DCs, $CD4^+$ and $CD8^+$ T cells, and $CD3^+$ $CD69^+$ T cells. For IHC analysis of infiltration cells, tumorswere harvested at day 20. Serial 5-μm-thick cryostat sections were prepared as described above and incubated with monoclonal antibodies (MAbs)

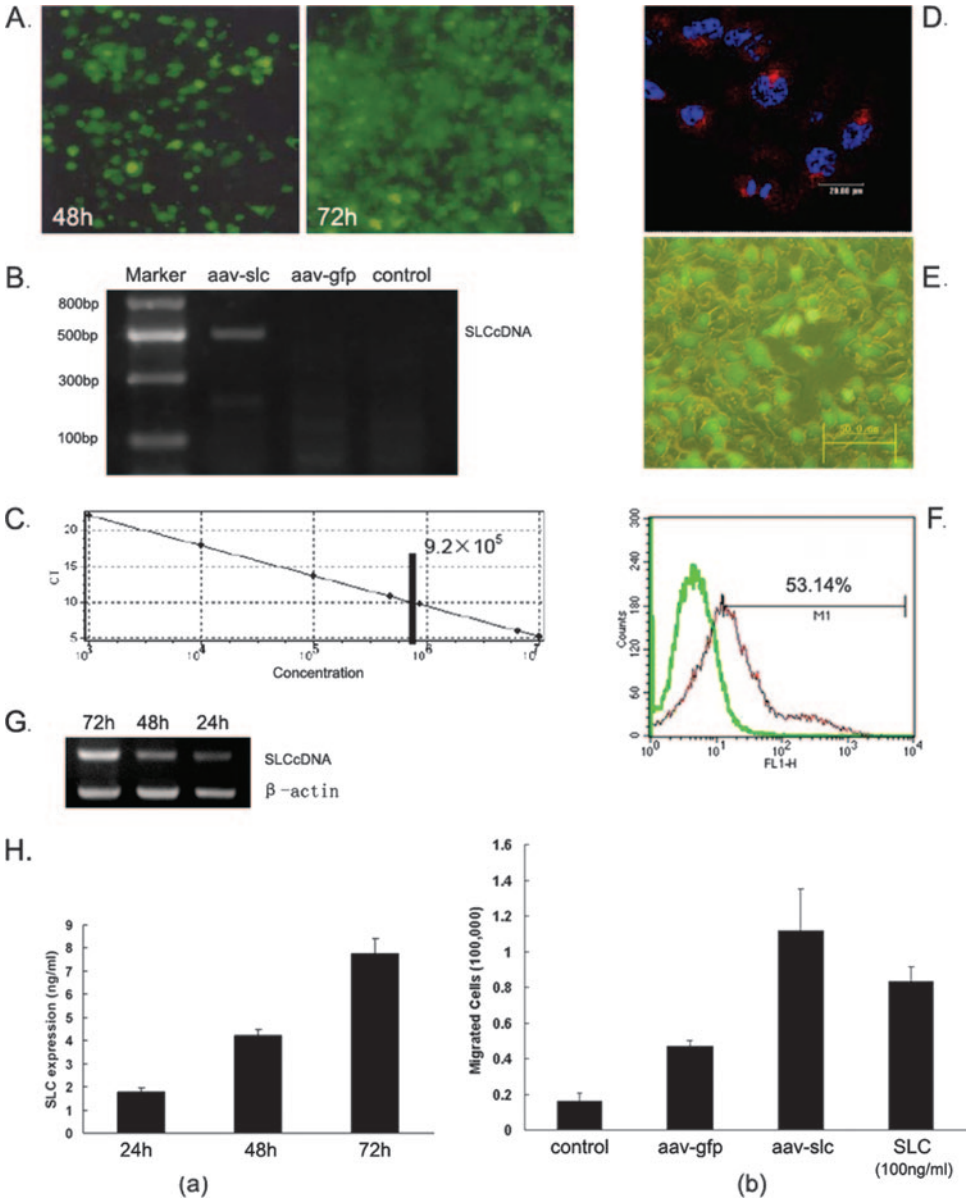

FIG. 1. rAAV-SLC virus was constructed and used to transduce Hepal-6 cells at high efficiency. (A) rAAV-SLC was packaged in AAV293 cells using the three-plasmid cotransfection system. hrGFP expression was used as an expression marker for the inserted SLC gene. AAV293 cells expressed GFP 48 h posttransduction, but more GFP-positive AAV293 cells were observed 72 h postinfection. (B) The encoding of SLC in the rAAV genome was determined by PCR. To amplify the fragments containing the full SLC coding region, specific primers for murine SLC were used. About a 500-bp PCR product of SLC peptide was detected. (C) The genome titer of rAAV-SLC was assayed by real-time PCR titration using a CMV promoter-specific primer set. The standard curve allowed conversion of the data points in the rAAV2-SLC (1 pg DNA is equivalent to 1.3×10^5 particles). The genome titer of rAAV-SLC is calculated as $(9.2 \times 10^5) \times (1.3 \times 10^5)$, or 1.25×10^{11} particles. (D) The distribution of Cy3-AAV-SLC particles (red) in Hepal-6 cells 2 h postinfection was observed to shift toward the nucleus and accumulate at the nuclear envelope. Hepal-6 cells were pulse labeled with particles of Cy3-rAAV-SLC particles for 10 min at 37°C, washed with serum-free RPMI 1640 medium to remove noninternalized virus, and then incubated at 37°C for 2 h prior to analysis by laser scanning confocal microscopy. Nuclei were assessed by DAPI (blue) staining. A representative image is shown, consisting of a single plane of focus through the center of a cell. (E) At 72 h postinfection, rAAV-SLC-mediated gene expression in Hepal-6 cells was analyzed by fluorescence microscopy for GFP fluorescence. (F) At 72 h postinfection, Hepal-6 cells were analyzed by fluorescence-activated cell sorting. More than 50% of the Hepal-6 cells were GFP positive. (G) The expression of SLC in Hepal-6 cells at 24, 48, and 72 h postinfection was determined by RT-PCR. (H) The SLC peptide concentration in supernatants was examined by SLC-specific ELISA. Supernatants from infected Hepal-6 cells were harvested at 24, 48, and 72 h postinfection. The standard curve was used in determining SLC concentrations in the supernatants (graph a). The bioactivity of SLC was confirmed by a chemotaxis assay. Supernatants from infected Hepal-6 cells 48 h postinfection were used in the bottom chamber of a 24-well plate for the chemotaxis assay. Recombinant SLC (100 ng/ml) was used to generate a standard control (graph b).

recognizing $CD4^+$, $CD8^+$ T cells, and $CD11c^+$ DCs (PharMingen, San Diego, CA). In order to determine the bioactivity of T cells, sections were also double stained with anti-CD3 and anti-CD69 (PharMingen, San Diego, CA). Isotype-matched antibodies were used as a control.

For flow cytometry analysis of effector cell infiltration, the remaining tumor samples were digested in 1 mg/ml type IV collagenase (Sigma, St. Louis, MO). Digested tumors were passed through a 70-μm-pore-size nylon mesh, washed once with Hank's balanced salt solution, and resuspended in PBS–3% bovine serum albumin to 1×10^6 cells/ml approximately. Samples were stained with fluorescein isothiocyanate (FITC)-conjugated antibodies to CD11c and CD3 and phycoerythrin (PE)-conjugated antibodies to CD4, CD8, and CD69 and then analyzed by flow cytometry.

The effect of rAAV-SLC on tumors established in nude mice. Hepal-6 cells were cultured and infected with rAAV-SLC or rAAV-GFP particles or noninfected and subsequently injected s.c. (10^6 cells/200 μl) into the right and/or left flank of 6- to 8-week-old nude mice. Developing tumors were monitored twice weekly as described above. Tumors were harvested at day 20, weighed and embedded in OCT compound before being snap frozen, and then stained for IHC analysis as described above. Serial cryostat sections were incubated with a rat MAb specific for CD31/platelet endothelial cell adhesion molecule 1 (PECAM-1) (1:50 dilution; PharMingen, San Diego, CA). Slides were subsequently washed and incubated with biotin-conjugated goat anti-rat immunoglobulin G (1:100 dilution; PharMingen, San Diego, CA) for 1 h at room temperature. Binding sites were detected with Cy3-coupled streptavidin. Based on the assay for intratumoral microvessel density (IMVD) reported by Weidner et al. (48), the 10 most vascular areas within a section were selected for quantization of angiogenesis. Vessels labeled with anti-CD31 MAb were counted under a fluorescence microscope at a magnification of ×200. The average counts were recorded as the CD31-IMVD.

Statistical analysis. For comparisons of two treatment groups, a Student's *t* test was performed. All statistical analyses were performed using SPSS software, version 12.0(Chicago, IL). Statistical significance was achieved at a P value of <0.05.

RESULTS

High transduction efficiency of liver cancer cells using rAAV2-SLC. A new rAAV2 encoding SLC was packaged in AAV293 cells (Fig. 1A) and harvested 72 h posttransfection. The correct encoding of SLC into the rAAV2 genome was determined by PCR (Fig. 1B). The virus titer was 1.25×10^{11} as analyzed by real-time PCR (Fig. 1C). Hepal-6 cells are highly susceptible to rAAV2-mediated gene transduction. At 2 h postinfection, the viral particles were observed to move toward the nucleus and to begin to accumulate at the nuclear envelope (Fig. 1D). At 72 h postinfection, rAAV-mediated gene expression in Hepal-6 cells was analyzed by fluorescence microscopy for GFP fluorescence (Fig. 1E). To estimate the percentage of transduced cells, fluorescence flow cytometry of GFP was used. The efficiency of transduction was greater than 50%, based on the number of GFP-positive cells. An example of this high-percentage transduction is presented in Fig. 1F. There was no difference in transduction efficiencies between the rAAV2-SLC and rAAV2-GFP viruses (data not shown).

SLC expression by Hepal-6 cells at 24, 48, and 72 h postinfection of rAAV2-SLC was confirmed by RT-PCR (Fig. 1.G). A specific ELISA was used to determine the level of SLC produced by rAAV2-SLC-expressing Hepal-6 cells. The standard curve was made with serial dilutions of the standard samples (1,000, 500, 250, 125, 62.5, 31.2, 15.6, and 7.8 pg/ml). Based on the standard curve, the absolute expression of SLC protein at different time points after the cells were transfected with rAAV2-SLC was calculated (Fig. 1H, graph a). A chemotaxis assay was used to further determine the levels and bioactivity of SLC produced in the supernatant of SLC-transduced Hepal-6 cells. As shown in Fig. 1H (graph b), the chemotactic activity of culture supernatants isolated from Hepal-6 cells 48 h postinfection with rAAV2-SLC was obviously stronger than that elicited by GFP-expressing Hepal-6 cells. The supernatants from GFP gene-modified Hepal-6 cells promoted chemotaxis of T cells to the same extent as that of culture supernatants from control Hepal-6 cells.

In order to determine whether the expression of SLC within the tumor cells is directly toxic to the cells, a viability stain was performed after transfection. Based on the exclusion of trypan blue dye from viable cells, there was no significant difference in the number of viable cells between groups (data not shown). The cell viability of transfected cells was further measured using an MTT assay. The data indicated that the proliferation indices were not affected in the different groups (24, 48, and 72 h posttransfection) (data not shown), suggesting that SLC expression itself has no effect on tumor viability.

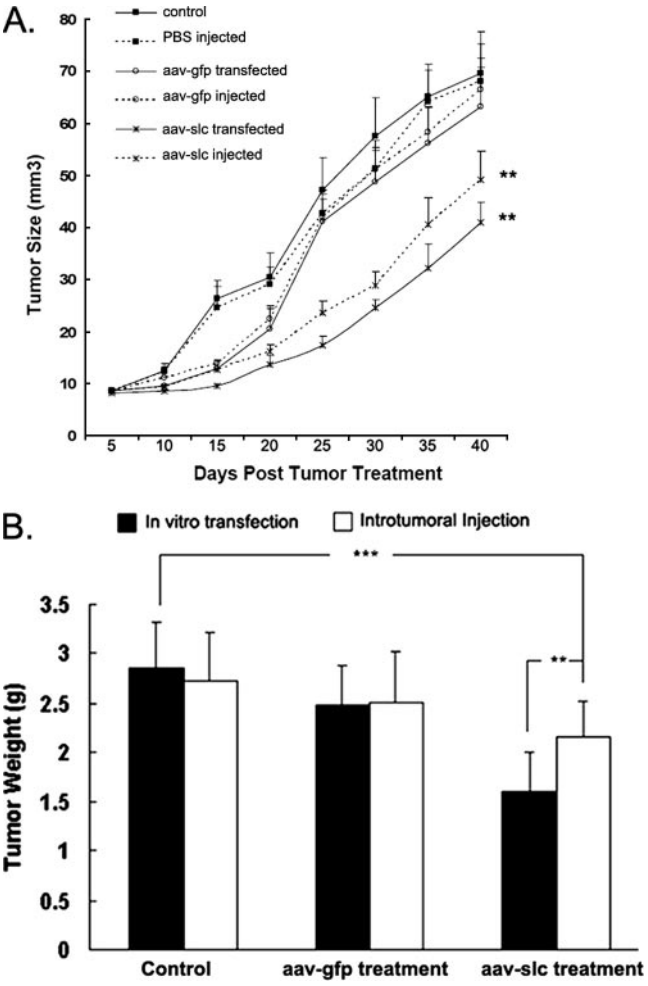

FIG. 2. rAAV-SLC promotes a potent antitumor effect. C57BL/6J mice were injected s.c with 1×10^6 Hepal-6 cells/200 μl that had already been transfected with rAAV-SLC or rAAV-GFP or left untreated as a control. After the tumors had grown to the size of 8 mm^3, control tumor-bearing mice also received three different treatments consisting of intratumoral injection with PBS, rAAV-GFP, or rAAV-SLC. Tumor size was monitored twice weekly. On day 40, all of the mice were sacrificed, and entire s.c. tumors were excised and weighed. (A) SLC-producing tumors showed a delayed progression compared with rAAV-GFP treatment. **, $P < 0.01$. No difference was observed between GFP-expressing and control or PBS background tumors. (B) rAAV-SLC-treated tumors were reduced in tumor weight. Between the two methods of virus treatment, in vitro transfection with rAAV-SLC showed more obvious inhibition in tumor growth than the direct in vivo intratumoral injection of rAAV-SLC. Bars indicate standard error. ***, $P < 0.001$; **, $P < 0.01$.

rAAV2-SLC induces a potent antitumor effect. The effect of SLC overexpression on antitumor immune responses was tested in tumor-bearing mouse models. C57BL/6J mice were injected s.c with Hepal-6 cells that had been previously transfected with either rAAV-SLC or rAAV-GFP or left untreated.

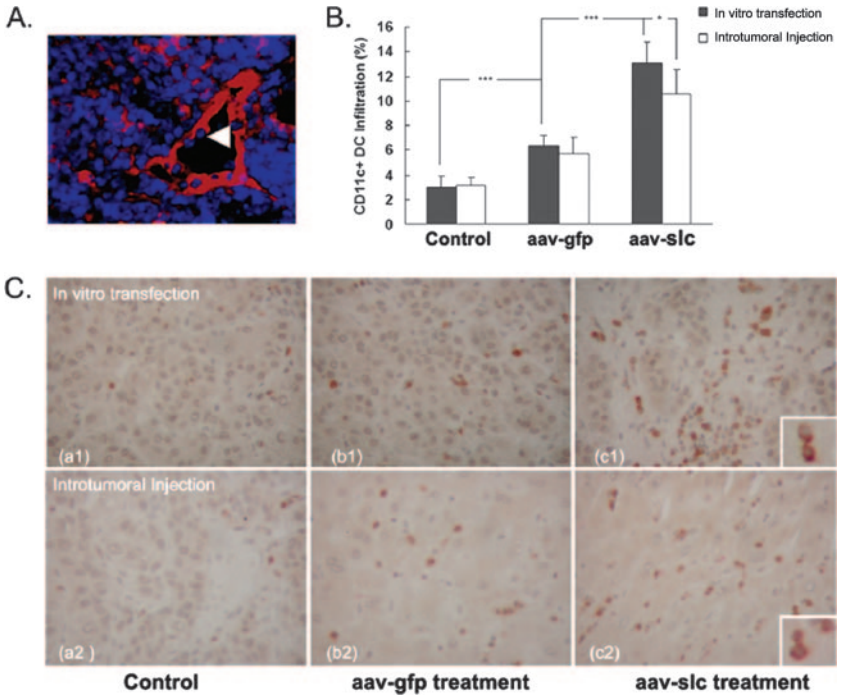

FIG. 3. Local expression of SLC attracted a heavy infiltration of immune effector cells and CD11c$^+$ DCs into tumors. C57BL/6J mice were injected s.c with Hepal-6 cells. On day 20, some mice were sacrificed, and the s.c. tumor was excised and partly embedded in OCT compound. (A) Serial 5-μm-thick cryostat sections from Hepal-6-implanted tumors were incubated with anti-murine SLC antibodies and amplified using a Cy3-streptavidin ABC system. HEVs and local expression of SLC (red) were indicated in tumors with rAAV-SLC treatment. Accumulated lymphocyte infiltrate (blue) was detected to form a new lymphoid-like tissue in established tumors. The infiltrating lymphocytes were observed to pass through the wall of the HEV (arrow). (B and C) Flow cytometry and IHC analysis showed more heavy infiltration of CD11c$^+$ DCs into the tumor sites. For flow cytometric analysis of CD11c$^+$ DC infiltration, the remaining tumor samples were digested with type IV collagenase and then stained with an FITC-conjugated antibody to CD11c. IHC analysis was able to detect CD11c$^+$ DCs recognized by diaminobenzidine staining (brown). Bars indicate standard error. ***, $P < 0.001$; *, $P < 0.05$.

rAAV-SLC-treated tumors showed a delayed progression compared to rAAV-GFP-treated tumors (Fig. 2A). Along with the reduction of growth, SLC overexpression also reduced tumor weight (Fig. 2B). In vivo a direct intratumoral injection of rAAV-SLC also inhibited tumor growth. However, the pretransduced tumor cells, which expressed SLC from the time of administration, displayed a stronger antitumor effect ($P < 0.01$). No difference was observed between rAAV-GFP-treated and normal background tumors as a result. However, it was shown that the tumor growth curve of the rAAV-GFP-treated group was not separated from the curve of the rAAV-SLC-treated group until about day 20.

Local expression of SLC promotes the recruitment of DCs and activated T cells to tumors in vivo. SLC expression was demonstrated by IHC analysis. HEVs and an accumulated lymphocyte infiltrate were found to form a lymphoid-like tissue in established tumors (Fig. 3A). Because SLC is chemotactic for both T cells and DCs, we hypothesized that SLC expressed by tumor cells would elicit migration of these cells to the tumor site. The infiltrating CD11c$^+$ DCs and CD4$^+$ and CD8$^+$ T cells were detected using both IHC analysis and flow cytometry. These analyses illustrated that significantly higher numbers of CD11c$^+$ DCs (Fig. 3B and C) and CD4$^+$ and CD8$^+$ T cells (Fig. 4) were recruited into tumors transduced with rAAV-SLC compared to the control and rAAV-GFP-treated tumors. A modest increase in immune cell density was also seen in rAAV-GFP-treated tumors, possibly because of an inflammatory immune reaction generated by rAAV-GFP infection. To quantify the activity of the infiltrated CD4$^+$ and CD8$^+$ T-cell lymphocytes, we analyzed cells by double staining with CD3 and CD69 by fluorescence-activated cell sorting analysis. We found that there were more CD3- and CD69-positive cells in tumors from the rAAV-SLC treatment group (Fig. 5). Taken together, these data show that rAAV-SLC treatment increases the number of DCs and activated T cells within the tumors.

Compared to the in vitro transfection treatment, a direct in vivo intratumoral injection of rAAV-SLC attracted significant infiltration of activated T cells and DCs. However, in this kind of treatment, there were fewer infiltrating effector cells, as shown in Fig. 4 ($P < 0.01$).

Inhibition of angiogenesis by rAAV-SLC in tumors in nude mice. To test whether SLC expression also induced antitumor activity apart from the anticipated immunological effects, we injected tumor cells with or without SLC treatment into nude mice. In general, the transplanted tumors in these animals grew significantly faster than in immunocompetent control animals, as there are no T cells to launch an antitumor immune response in vivo. However, despite the lack of a T-cell-mediated response, tumor weight was found to be significantly different from control animals (Fig. 6A). Quantification of IMVD was performed by CD31 staining and subsequent determination of IMVD in the 10 most vascularized areas within a sec-

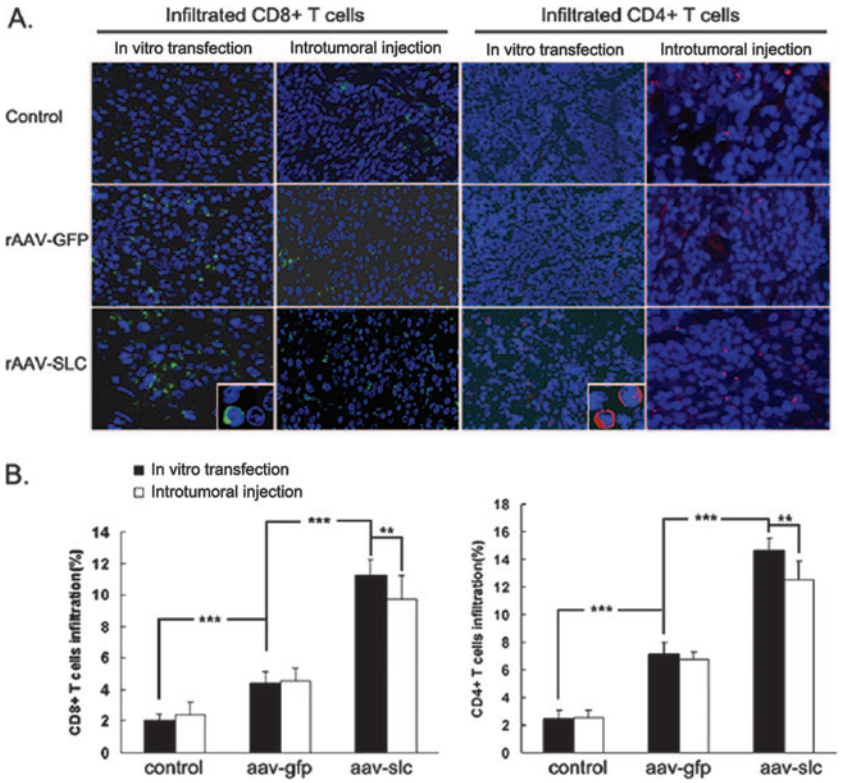

FIG. 4. rAAV-SLC enhances infiltration of $CD4^+$ and $CD8^+$ T cells into the tumor site. (A) IHC analysis for infiltrated $CD4^+$ and $CD8^+$ T cells in the tumors. Tumor sections were incubated with MAbs recognizing PE-$CD4^+$ and FITC-$CD8^+$ T cells. More PE-$CD4^+$ T cells (red) and FITC-$CD8^+$ T cells (green) were detected in rAAV-SLC-treated tumors. (B) To further quantify the number of infiltrating lymphocytes, tumor samples were digested with type IV collagenase. The collected cells were stained with FITC-anti-CD3 and PE-anti-CD4 or PE-anti-CD8 for flow cytometric evaluation. Compared with the control and rAAV-GFP-treated mice, significantly higher numbers of $CD4^+$ and $CD8^+$ T cells were found in the infiltrate of SLC-treated mice. Bars indicate standard error. ***, $P < 0.001$; **, $P < 0.01$.

tion. As shown in Fig. 6B and C, a decrease in CD31-IMVD was observed in tumors established from SLC-expressing Hepal-6 tumor cells. The difference between the two groups reached statistical significance ($P < 0.05$).

DISCUSSION

The induction of a potent antitumor immune response requires the fine-tuned choreography of multiple immune effector cell types, including APCs and different subsets of T cells. DCs, the most potent APCs, play a critical role in this process through a series of functions including antigen capture and processing, up-regulation of costimulatory signals, and finally antigen presentation and activation of T cells (2). Efficient retrieval and transport of DCs into T-cell-rich areas is primarily mediated by SLC (35) and ELC (1), which engage a single receptor, CCR7. Previous work demonstrated that the chemotactic activity of SLC for DCs and T cells could be harnessed to generate antitumor immune responses (24, 30, 37, 38, 44, 45). In light of these results, recent work by Flanagan et al. (11) showed that SLC costimulates naïve T-cell expansion and Th1 polarization of nonregulatory $CD4^+$ T cells. In other studies, SLC enhanced the immunity of an antimelanoma DNA vaccine (53) and was evaluated for antitumor effect by coexpression of SLC and the costimulatory molecule LIGHT (16). Almost all of these reports indicated that the antitumor effect of SLC was mediated by greatly enhancing the infiltration of mature DCs and $CD8^+$ T cells to the tumor. These data also suggested that modulation of the tumor microenvironment could lead to effective T-cell priming and the generation of functional antitumor effector cells in the absence of functional lymph nodes.

We reasoned that such an activity could be improved upon by in situ activation of recruited DCs and T cells via local long-term expression of SLC. In this study, we applied an rAAV vector to deliver SLC directly into the tumor cells. This choice was based on the broad host range, excellent safety profile, and the ability of rAAV to integrate into the host genome as well as to provide long-term expression in infected hosts (20, 52, 57). Although studies have addressed the efficacy of AAV-mediated gene therapy in different human and mammalian cell types, the most efficient vector transduction in vivo has been reported in skeletal muscle and brain, followed by hepatocytes (4, 22, 29, 52, 58). Subsequent to infection, AAV is transported to the nucleus within a short time, and uncoating of the capsid releases the vector genome into the host cell nucleus (3). Consistent with previous reports, we found that Cy3-conjugated AAV was bound to Hepal-6 cells and exhibited a dispersed, punctate distribution in the cell, likely reflecting virions in both endocytic compartments, and was free within the cytosol. Perinuclear accumulation was observed by

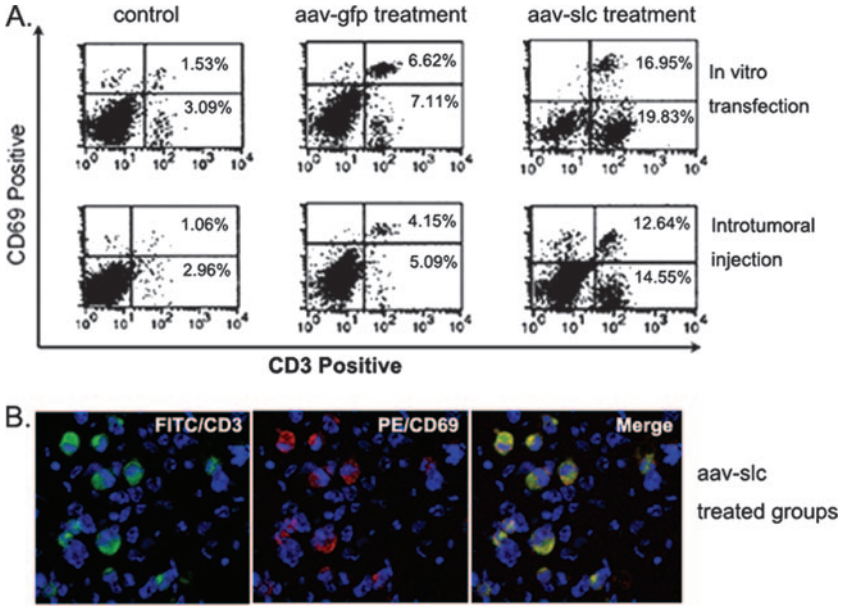

FIG. 5. The infiltrated T cells are mostly activated cells. In order to determine the bioactivity of the infiltrated T cells, the collected cells were also double stained with FITC-anti-CD3 and PE-anti-CD69. Isotype-matched antibodies were used as a control. In comparison with the control and rAAV-GFP treatment groups, significantly higher numbers of $CD3^+$ $CD69^+$ T cells were found in the infiltrate of SLC-treated mice by flow cytometric evaluation. Most CD3-positive T cells (green) are CD69 positive (red) in the rAAV-SLC-treated group and displayed double staining (yellow).

2 h. We demonstrated that Hepal-6 cells are highly susceptible to rAAV-mediated gene transduction in this study.

In contrast to other reports (37, 38, 54, 55), we harnessed the long-term, local expression of SLC in the tumor bed mediated by rAAV vector to detect its antitumor effect. Our results showed that rAAV-SLC was more effective in generating systemic antitumor responses, accompanied by extensive infiltration of $CD11c^+$ DCs and $CD4^+$ and $CD8^+$ T cells into the tumor site, especially activated $CD3^+$ $CD69^+$ T cells. HEV and a lymphocyte infiltrate were found to form a new lymphoid-like tissue within established tumors. These data suggest that long-term ectopic expression of SLC in tumors could trigger lymphoid neogenesis. It is well established that SLC (5, 13, 17, 28) is expressed predominantly in lymph node HEV, but it is also expressed by cells in the T-cell-dependent regions of lymphoid tissue. In the thymus, it is expressed by cells in the medulla, including blood vessels and medullary epithelium, and may contribute to tissue organization. For example, in the thymus, thymocytes and DCs acquire expression of the SLC receptor, CCR7, during development (21, 43); therefore, medullary expression of SLC may induce migration of mature cells toward the medulla. Similarly, expression of SLC by HEV may help organize the T-cell/DC compartment around HEV, whereas an opposing gradient of the chemokine, B-lymphocyte chemoattractant, produced by follicular DC, draws B cells into the B-cell follicles. To assess the role of SLC in lymphoid tissue development, Fan et al. (10) generated transgenic mice with islet β-cell-specific expression of SLC and found that ectopic expression of the SLC is sufficient to trigger lymphoid neogenesis by recruiting the lymphocytes and DCs to pancreatic islets. Thus, our present result is coincident with previous studies. On the other hand, this result also suggested that local expression of SLC in the tumor bed might play another role in the antitumor effect by destroying the solid tumor barrier through recruitment of the extensive, activated $CD4^+$ and $CD8^+$ T cells, as well as $CD11c^+$ DCs.

The "barrier" formed around solid tumors by infiltrating host stroma hinders the presentation of tumor antigens in draining lymph nodes, and, in the absence of a robust costimulatory environment, specific T cells can remain ignorant or become energized (31, 32). Additional obstacles for T-cell homing and expansion inside tumors may also hinder tumor eradication (49). Murine models have shown that abundant, activated, tumor antigen-specific T cells fail to reject tumors even when they can reject skin grafts or less established tumors bearing the same antigen (14). Thus, the tumor barrier may be an important contributor to the failure of tumor rejection. However, it is possible that the active recruitment of naive T cells into tumors, followed by their activation through robust costimulation and sufficient antigen load, may overcome these obstacles to antitumor immunity. So, targeting the tumor barrier might indeed be useful for immunotherapy. In this study, we also observed some lymphocytes passing through the wall of the HEV, which was hypothesized to contribute in destroying the tumor barrier.

In addition to CCR7, mouse SLC has also been shown to signal through mouse CXCR3 and share some of the activities of gamma interferon-inducible protein 10 and monokine induced by gamma interferon (19). As CD31/PECAM-1 has been proved to be involved in angiogenesis by previous works (8, 40), we selected CD31 expression as a marker of angiogenesis in SLC-treated tumors that were established in nude mice. As a result, the mechanism underlying the antitumor effect of rAAV-SLC was further ex-

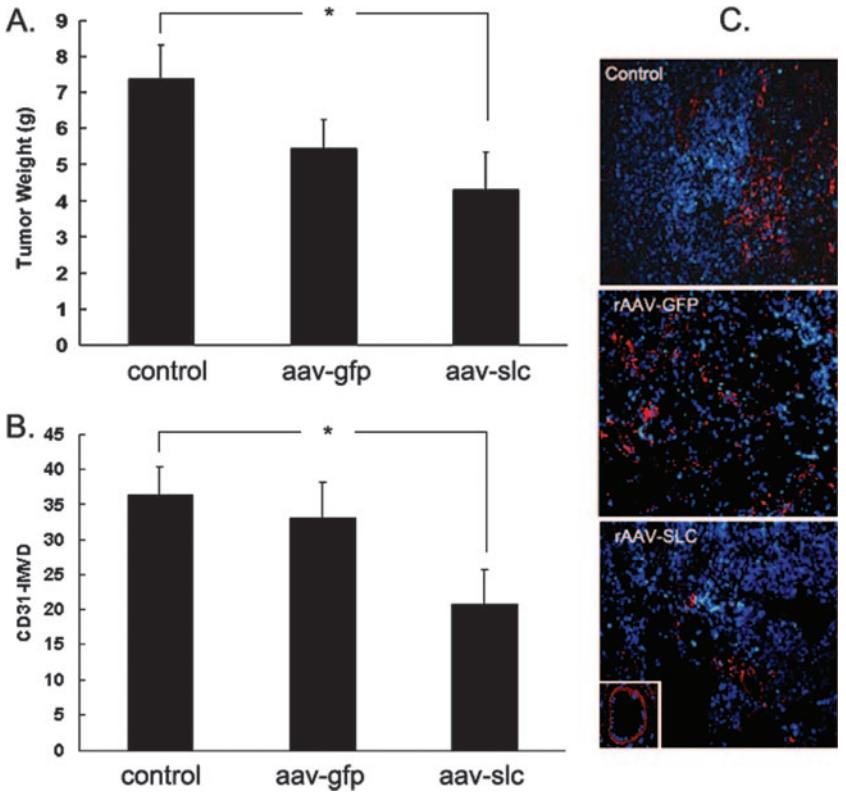

FIG. 6. Local expression of SLC inhibits angiogenesis of tumors. Nude mice were injected s.c with 1×10^6 Hepal-6 cells/200 μl, with or without SLC treatment. On day 20, all the mice were sacrificed, and the tumors were excised and embedded in OCT compound for serial 5-μm-thick cryostat sections. (A) Tumor weight in the SLC-treated group was significantly lower than that of wild-type animals. *, $P < 0.05$. (B and C) Quantification of IMVD was performed by CD31 staining and subsequent determination of IMVD in the 10 most vascularized areas within a section. For each section, the positive data were calculated automatically by computer software. An antibody specific for CD31 was used as the first antibody and amplified using the Cy3-streptavidin ABC system. A decrease in CD31-IMVD was observed in tumors established from SLC-expressing Hepal-6 tumor cells. The difference between the two groups reached statistical significance (*, $P < 0.05$). Bars indicate standard error.

amined and elucidated in detail, revealing that local expression of SLC also plays an important role in the inhibition of neoangiogenesis in the tumor bed. Is the protection by SLC in wild-type mice due to an increased T-cell response or due to the inhibition of angiogenesis? We believe that the protection by SLC in wild-type mice is mainly due to an increased T-cell response. This point was demonstrated in our preliminary experiments by using pertussis toxin (a specific inhibitor of CCR7) to block the infiltration of immune effector cells, and we found a poorer antitumor effect, compared to that without pertussis toxin treatment (data not shown). However, we also believe the inhibition of angiogenesis would play an important role in the antitumoral effect as time went on, which could be inferred from the rAAV-GFP-treated groups. In this study we also found that GFP-AAV has some effects on DC and T-cell infiltration. The effects are likely due to an inflammatory immune reaction generated by rAAV2 itself. This result is consistent with a recent study (46), indicating that AAV2 capsid proteins can elicit primary cellular immune responses when injected into the skeletal muscle. So the increased infiltration of effector cells in the rAAV-GFP-treated group could explain the result that its tumor growth curve was not separated from the curve of rAAV-SLC-treated group until about day 20. As time went on, the tumor microenvironment (such as the secretion of transforming growth facto β and interleukin-10) might educate T cells into regulatory T cells, or more and more T cells would become ignorant. This might be the reason why there was no observed difference in antitumoral effect between rAAV-GFP-treated and normal background tumors. As to rAAV-SLC-treated tumors, it could be inferred that the inhibition effect of angiogenesis would play a main role from then on. Additional studies will be required to delineate these properties of rAAV-SLC and effector T cells as well as the tumor microenvironment in vivo.

Overall, these results suggest that mouse SLC gene transfer into a liver cancer cell line by rAAV transduction elicits strong antitumor effects by inducing both an angiostatic effect and lymphocyte infiltration, as well as destruction of the tumor barrier. In summary, our work outlines a comprehensive immune therapy strategy applicable for solid tumors based on cooperative interaction of multiple effector cell types. This strategy may overcome the functional immune impairment observed in patients with advanced malignancy. The results also throw some light on studies about the tumor microenvironment and T cells.

ACKNOWLEDGMENTS

We thank Dominik Wolf from the Medical University Innsbruck and Zhang Su-chun from the University of Wisconsin—Madison for critical readings and comments.

This work was supported by grants from the State Key Basic Research Program of China (grants G1998051210 and 2004CB518708) and from the National Science Foundation of China (grants 30500280 and 30370748).

REFERENCES

1. **Baekkevold, E. S., T. Yamanaka, R. T. Palframan, H. S. Carlsen, F. P. Reinholt, U. H. von Andrian, P. Brandtzaeg, and G. Haraldsen.** 2001. The CCR7 ligand ELC (CCL19) is transcytosed in high endothelial venules and mediates T cell recruitment. J. Exp. Med. **193:**1105–1112.
2. **Banchereau, J., and R. M. Steinman.** 1998. Dendritic cells and the control of immunity. Nature **392:**245–252.
3. **Bartlett, J. S., R. Wilcher, and R. J. Samulski.** 2000. Infectious entry pathway of adeno-associated virus and adeno-associated virus vectors. J. Virol. **74:** 2777–2785.
4. **Bjorklund, A., D. Kirik, C. Rosenblad, B. Georgievska, C. Lundberg, and R. J. Mandel.** 2000. Towards a neuroprotective gene therapy for Parkinson's disease: use of adenovirus, AAV and lentivirus vectors for gene transfer of GDNF to the nigrostriatal system in the rat Parkinson model. Brain Res. **886:**82–98.
5. **Campbell, J. J., E. P. Bowman, K. Murphy, K. R. Youngman, M. A. Siani, D. A. Thompson, L.Wu, A. Zlotnik, and E. C. Butcher.** 1998. 6-C-kine (SLC), a lymphocyte adhesion-triggering chemokine expressed by high endothelium, is an agonist for the MIP-3beta receptor CCR7. J. Cell Biol. **141:**1053–1059.
6. **Chan, V. W., S. Kothakota, M. C. Rohan, L. Panganiban-Lustan, J. P. Gardner, M. S. Wachowicz, J. A. Winter, and L. T. Williams.** 1999. Secondary lymphoid-tissue chemokine (SLC) is chemotactic for mature dendritic cells. Blood **93:**3610–3616.
7. **Cukor, G., N. R. Blacklow, S. Kibrick, and I. C. Swan.** 1975. Effect of adeno-associated virus on cancer expression by herpesvirus-transformed hamster cells. J. Natl. Cancer Inst. **55:**957–959.
8. **DeLisser, H. M., M. Christofidou-Solomidou, R. M. Strieter, M. D. Burdick, C. S. Robinson, R. S. Wexler, J. S. Kerr, C. Garlanda, J. R. Merwin, J. A. Madri, and S. M. Albelda.** 1997. Involvement of endothelial PECAM-1/CD31 in angiogenesis. Am. J. Pathol. **151:**671–677.
9. **During, M. J., R. J. Samulski, J. D. Elsworth, M. G. Kaplitt, P. Leone, X. Xiao, J. Li, A. Freese, J. R. Taylor, R. H. Roth, J. R. Sladek, Jr., K. L. O'Malley, and D. E. Redmond, Jr.** 1998. In vivo expression of therapeutic human genes for dopamine production in the caudates of MPTP-treated monkeys using an AAV vector. Gene Ther. **5:**820–827.
10. **Fan, L., C. R. Reilly, Y. Luo, M. E. Dorf, and D. Lo.** 2000. Cutting edge: ectopic expression of the chemokine TCA4/SLC is sufficient to trigger lymphoid neogenesis. J. Immunol. **164:**3955–3959.
11. **Flanagan, K., D. Moroziewicz, H. Kwak, H. Horig, and H. L. Kaufman.** 2004. The lymphoid chemokine CCL21 costimulates naive T cell expansion and Th1 polarization of non-regulatory CD4+ T cells. Cell Immunol. **231:**75–84.
12. **Gunn, M. D., S. Kyuwa, C. Tam, T. Kakiuchi, A. Matsuzawa, L. T. Williams, and H. Nakano.** 1999. Mice lacking expression of secondary lymphoid organ chemokine have defects in lymphocyte homing and dendritic cell localization. J. Exp. Med. **289:**451–460.
13. **Gunn, M. D., K. Tangemann, C. T am, J. G. Cyster, S. D. Rosen, and L. T. Williams.** 1998. A chemokine expressed in lymphoid high endothelial venules promotes the adhesion and chemotaxis of naive T lymphocytes. Proc. Natl. Acad. Sci. USA **95:**258–263.
14. **Hanson, H. L., D. L. Donermeyer, H. Ikeda, J. M. White, V. Shankaran, L. J. Old, H. Shiku, R. D. Schreiber, and P. M. Allen.** 2000. Eradication of established tumors by CD8+ T cell adoptive immunotherapy. Immunity **13:**265–276.
15. **Hermonat, P. L.** 1994. Adeno-associated virus inhibits human papillomavirus type 16: a viral interaction implicated in cervical cancer. Cancer Res. **54:** 2278–2281.
16. **Hisada, M., T. Yoshimoto, S. Kamiya, Y. Magami, H. Miyaji, T. Yoneto, K. Tamada, T. Aoki, Y. Koyanagi, and J. Mizuguchi.** 2004. Synergistic antitumor effect by coexpression of chemokine CCL21/SLC and costimulatory molecule LIGHT. Cancer Gene Ther. **11:**280–288.
17. **Hromas, R., C. H. Kim, M. Klemsz, M. Krathwohl, K. Fife, S. Cooper, C. Schnizlein-Bick, and H. E. Broxmeyer.** 1997. Isolation and characterization of Exodus-2, a novel C-C chemokine with a unique 37-amino acid carboxyl-terminal extension. J. Immunol. **159:**2554–2558.
18. **Huang, A. Y., P. Golumbek, M. Ahmadzadeh, E. Jaffee, D. Pardoll, and H. Levitsky.** 1994. Role of bone marrow-derived cells in presenting MHC class I-restricted tumor antigens. Science **264:**961–965.
19. **Jenh, C. H., M. A. Cox, H. Kaminski, M. Zhang, H. Byrnes, J. Fine, D. Lundell, C. C. Chou, S. K. Narula, and P. J. Zavodny.** 1999. Cutting edge: species specificity of the CC chemokine 6Ckine signaling through the CXC chemokine receptor CXCR3: human 6Ckine is not a ligand for the human or mouse CXCR3 receptors. J. Immunol. **162:**3765–3769.
20. **Kaplitt, M. G., P. Leone, R. J. Samulski, X. Xiao, D. W. Pfaff, K. L. O'Malley, and M. J. During.** 1994. Long-term gene expression and phenotypic correction using adeno-associated virus vectors in the mammalian brain. Nat. Genet. **8:**148–154.
21. **Kellermann, S. A., S. Hudak, E. R. Oldham, Y. J. Liu, and L. M. McEvoy.** 1999. The CC chemokine receptor-7 ligands 6Ckine and macrophage inflammatory protein-3 beta are potent chemoattractants for in vitro- and in vivo-derived dendritic cells. J. Immunol. **162:**3859–3864.
22. **Kessler, P. D., G. M. Podsakoff, X. Chen, S. A. McQuiston, P. C. Colosi, L. A. Matelis, G. J. Kurtzman, and B. J. Byrne.** 1996. Gene delivery to skeletal muscle results in sustained expression and systemic delivery of a therapeutic protein. Proc. Natl. Acad. Sci. USA **93:**14082–14087.
23. **Kim, C. H., L. M. Pelus, E. Appelbaum, K. Johanson, N. Anzai, and H. E. Broxmeyer.** 1999. CCR7 ligands, SLC/6Ckine/Exodus2/TCA4 and CKbeta-11/MIP-3beta/ELC, are chemoattractants for CD56(+)CD16(−) NK cells and late stage lymphoid progenitors. Cell Immunol. **193:**226–235.
24. **Kirk, C. J., D. Hartigan-O'Connor, B. J. Nickoloff, J. S. Chamberlain, M. Giedlin, L. Aukerman, and J. J. Mule.** 2001. T cell-dependent antitumor immunity mediated by secondary lymphoid tissue chemokine: augmentation of dendritic cell-based immunotherapy. Cancer Res. **61:**2062–2070.
25. **Lee, H. C., S. J. Kim, K. S. Kim, H. C. Shin, and J. W. Yoon.** 2000. Remission in models of type 1 diabetes by gene therapy using a single-chain insulin analogue. Nature **408:**483–488.
26. **Matsushita, T., S. Elliger, C. Elliger, G. Podsakoff, L. Villarreal, G. J. Kurtzman, Y. Iwaki, and P. Colosi.** 1998. Adeno-associated virus vectors can be efficiently produced without helper virus. Gene Ther. **5:**938–945.
27. **Nagira, M., T. Imai, R. Yoshida, S. Takagi, M. Iwasaki, M. Baba, Y. Tabira, J. Akagi, H. Nomiyama, and O. Yoshie.** 1998. A lymphocyte-specific CC chemokine, secondary lymphoid tissue chemokine (SLC), is a highly efficient chemoattractant for B cells and activated T cells. Eur. J. Immunol. **28:**1516–1523.
28. **Nagira, M., T. Imai, K. Hieshima, J. Kusuda, M. Ridanpaa, S. Takagi, M. Nishimura, M. Kakizaki, H. Nomiyama, and O. Yoshie.** 1997. Molecular cloning of a novel human CC chemokine secondary lymphoid-tissue chemokine that is a potent chemoattractant for lymphocytes and mapped to chromosome 9p13. J. Biol. Chem. **272:**19518–19524.
29. **Nakai, H., E. Montini, S. Fuess, T. A. Storm, M. Grompe, and M. A. Kay.** 2003. AAV serotype 2 vectors preferentially integrate into active genes in mice. Nat. Genet. **34:**297–302.
30. **Nomura, T., H. Hasegawa, M. Kohno, M. Sasaki, and S. Fujita.** 2001. Enhancement of anti-tumor immunity by tumor cells transfected with the secondary lymphoid tissue chemokine EBI-1-ligand chemokine and stromal cell-derived factor-1α chemokine genes. Int. J. Cancer **91:**597–606.
31. **Ochsenbein, A. F., P. Klenerman, U. Karrer, B. Ludewig, M. Pericin, H. Hengartner, and R. M. Zinkernagel.** 1999. Immune surveillance against a solid tumor fails because of immunological ignorance. Proc. Natl. Acad. Sci. USA **96:**2233–2238.
32. **Ochsenbein, A. F., S. Sierro, B. Odermatt, M. Pericin, U. Karrer, J. Hermans, S. Hemmi, H. Hengartner, and R. M. Zinkernagel.** 2001. Roles of tumour localization, second signals and cross priming in cytotoxic T-cell induction. Nature **411:**1058–1064.
33. **Pachynski, R. K., S. W. Wu, M. D. Gunn, and D. J. Erle.** 1998. Secondary lymphoid-tissue chemokine (SLC) stimulates integrin alpha 4 beta 7-mediated adhesion of lymphocytes to mucosal addressin cell adhesion molecule-1 (MAdCAM-1) under flow. J. Immunol. **161:**952–956.
34. **Rohr, U. P., M. A. Wulf, S. Stahn, U. Steidl, R. Haas, and R. Kronenwett.** 2002. Fast and reliable titration of recombinant adeno-associated virus type-2 using quantitative real-time PCR. J. Virol. Methods **106:**81–88.
35. **Saeki, H., A. Moore, M. Brown, and S. Hwang.** 1999. Cutting edge: secondary lymphoid-tissue chemokine (SLC) and CC chemokine receptor 7 (CCR7) participate in the emigration pathway of mature dendritic cells from the skin to regional lymph nodes. J. Immunol. **162:**2472–2475.
36. **Sanlioglu, S., P. Benson, and J. F. Engelhardt.** 2000. Loss of ATM function enhances recombinant adeno-associated virus transduction and integration through pathways similar to UV irradiation. Virology **268:**68–78.
37. **Sharma, S., M. Stolina, L. Zhu, Y. Lin, R. Batra, M. Huang, R. Strieter, and S. M. Dubinett.** 2001. Secondary lymphoid organ chemokine reduces pulmonary tumor burden in spontaneous murine bronchoalveolar cell carcinoma. Cancer Res. **61:**6406–6412.
38. **Sharma, S., M. Stolina, J. Luo, R. M. Strieter, M. Burdick, L. X. Zhu, R. K. Batra, and S. M. Dubinett.** 2000. Secondary lymphoid tissue chemokine mediates T cell-dependent antitumor responses in vivo. J. Immunol. **164:** 4558–4563.
39. **Sharma, S., S. C. Yang, S. Hillinger, L. X. Zhu, M. Huang, R. K. Batra, J. F. Lin, M. D. Burdick, R. M. Strieter, and S. M. Dubinett.** 15 April 2003, posting date. SLC/CCL21-mediated anti-tumor responses require IFN-gamma, MIG/CXCL9 and IP-10/CXCL10. Mol. Cancer **2:**22. doi:10.1186/1476-4598-2-22.
40. **Solowiej, A., P. Biswas, D. G raesser, and J. A. Madri.** 2003. Lack of platelet

endothelial cell adhesion molecule-1 attenuates foreign body inflammation because of decreased angiogenesis. Am. J. Pathol. **162:**953–962.

41. **Soto, H., W. Wang, R. M. Strieter, N. G. Copeland, D. J. Gilbert, N. A. Jenkins, J. Hedrick, and A. Zlotnik.** 1998. The CC chemokine 6Ckine binds the CXC chemokine receptor CXCR3. Proc. Natl. Acad. Sci. USA **95:**8205–8210.
42. **Su, H., S. Joho, Y. Huang, A. Barcena, J. Arakawa-Hoyt, W. Grossman, and Y. W. Kan.** 2004. Adeno-associated viral vector delivers cardiac-specific and hypoxia-inducible VEGF expression in ischemic mouse hearts. Proc. Natl. Acad. Sci. USA **101:**16280–16285.
43. **Suzuki, G., H. Sawa, Y. Kobayashi, Y. Nakata, K. Nakagawa, A. Uzawa, H. Sakiyama, S. Kakinuma, K. Iwabuchi, and K. Nagashima.** 1999. Pertussis toxin-sensitive signal controls the trafficking of thymocytes across the corticomedullary junction in the thymus. J. Immunol. **162:**5981–5985.
44. **Tolba, K. A., W. J. Bowers, J. Muller, V. Houseknecht, R. E. Giuliano, H. J. Federoff, and J. D. Rosenblatt.** 2002. Herpes simplex virus (HSV) amplicon-mediated codelivery of secondary lymphoid tissue chemokine and CD40L results in augmented antitumor activity. Cancer Res. **62:**6545–6551.
45. **Vicari, A. P., S. A. Yahia, K. Chemin, A. Mueller, A. Zlotnik, and C. Caux.** 2000. Antitumor effects of the mouse chemokine 6Ckine/SLC through angiostatic and immunological mechanisms. J. Immunol. **165:**1992–2000.
46. **Wang, Z., J. M. Allen, S. R. Riddell, P. Gregorevic, R. Storb, S. J. Tapscott, J. S. Chamberlain, and C. S. Kuhr.** 2007. Immunity to adeno-associated virus-mediated gene transfer in a random-bred canine model of Duchenne muscular dystrophy. Hum. Gene Ther. **18:**18–26.
47. **Warren, P., W. Song, E. Holle, L. Holmes, Y. Wei, J. Li, T. Wagner, and X. Yu.** 2002. Combined HSV-TK/GCV and secondary lymphoid tissue chemokine gene therapy inhibits tumor growth and elicits potent antitumor CTL response in tumor-bearing mice. Anticancer Res. **22:**599–604.
48. **Weidner, N., J. P. Semple, and W. R. Welch.** 1991. Tumor angiogenesis and metastasis 2 correlation in invasive breast carcinoma. N. Engl. J. Med. **324:**1–8.
49. **Wick, M., P. Dubey, H. Koeppen, C. T. Siegel, P. E. Fields, L. Chen, J. A. Bluestone, and H. Schreiber.** 1997. Antigenic cancer cells grow progressively in immune hosts without evidence for T cell exhaustion or systemic anergy. J. Exp. Med. **186:**229–238.
50. **Willimann, K., D. F. Legler, M. Loetscher, R. S. Roos, M. B. Delgado, I. Clark-Lewis, M. Baggiolini, and B. Moser.** 1998. The chemokine SLC is expressed in T cell areas of lymph nodes and mucosal lymphoid tissues and attracts activated T cells via CCR7. Eur. J. Immunol. **28:**2025–2034.
51. **Wu, F. Y., C. Y. Wu, C. H. Lin, and C. H. Wu.** 1999. Suppression of tumorigenicity in cervical carcinoma HeLa cells by an episomal form of adeno-associated virus. Int. J. Oncol. **15:**101–106.
52. **Xu, R., X. Sun, L. Y. Tse, H. Li, P. C. Chan, S. Xu, W. Xiao, H. F. Kung, G. W. Krissansen, and S. T. Fan.** 2003. Long-term expression of angiostatin suppresses metastatic liver cancer in mice. Hepatology **37:**1451–1460.
53. **Yamano, T., Y. Kaneda, S. Huang, S. H. Hiramatsu, and D. S. Hoon.** 2006. Enhancement of immunity by a DNA melanoma vaccine against TRP2 with CCL21 as an adjuvant. Mol. Ther. **13:**194–202.
54. **Yang, S. C., R. K. Batra, S. Hillinger, K. L. Reckamp, R. M. Strieter, S. M. Dubinett, and S. Sharma.** 2006. Intrapulmonary administration of CCL21 gene-modified dendritic cells reduces tumor burden in spontaneous murine bronchoalveolar cell carcinoma. Cancer Res. **66:**3205–3213.
55. **Yang, S. C., S. Hillinger, K. Riedl, L. Zhang, L. Zhu, M. Huang, K. Atianzar, B. Y. Kuo, B. Gardner, R. K. Batra, R. M. Strieter, S. M. Dubinett, and S. Sharma.** 2004. Intratumoral administration of dendritic cells overexpressing CCL21 generates systemic antitumor responses and confers tumor immunity. Clin. Cancer Res. **10:**2891–2901.
56. **Yoshida, R., M. Nagira, M. Kitaura, N. Imagawa, T. Imai, and O. Yoshie.** 1998. Secondary lymphoid-tissue chemokine is a functional ligand for the CC chemokine receptor CCR7. J. Biol. Chem. **273:**7118–7122.
57. **Zhang, F., C. L. Chen, J. Q. Qian, J. T. Yan, K. Cianflone, X. Xiao, and D. W. Wang.** 2005. Long-term modifications of blood pressure in normotensive and spontaneously hypertensive rats by gene delivery of rAAV-mediated cytochrome P450 arachidonic acid hydroxylase. Cell Res. **15:**717–724.
58. **Zhong, L., W. Li, Z. Yang, L. Chen, Y. Li, K. Qing, K. A. Weigel-Kelley, M. C. Yoder, W. Shou, and A. Srivastava.** 2004. Improved transduction of primary murine hepatocytes by recombinant adeno-associated virus 2 vectors in vivo. Gene Ther. **11:**1165–1169.